Geant4 and Fano cavity : where are we ?

S. Elles, V. Ivanchenko, M. Maire, L. Urban

Geant4 and Fano cavity test: where are we?

S Elles[1], V N Ivanchenko[2,3], M Maire[1], L Urban[4]
[1] LAPP, Annecy-le-Vieux, France
[2] CERN, Geneva, Switzerland
[3] EMSU, Moscow, Russia
[4] RMKI, Budapest, Hungary

Abstract. The electron transport algorithm implemented in Geant4 has been recently revised. The modifications concern several physics aspects of the simulation model: the step limitation, the energy loss along a step and the multiple scattering. The Fano cavity setup was used to test these developments. The upgrades increase significantly the accuracy of the electron transport simulation. The ratio of simulated to theoretical dose deposition in the cavity is stable to ~1% while varying several parameters and within ~1.5% of the expected value for water and graphite. Work is underway to identify and resolve the remaining shift.

1. Introduction

The simulation of ionization chambers is known as a stringent test for condensed history electron transport in Monte Carlo codes [1]. E. Poon et al [2] have investigated the capability of an earlier release of the Geant4 toolkit [3], version 6.2.p01, for such setups and demonstrated a strong step size dependence of the cavity dose deposition calculation.

This note provides a summary of the revisions undertaken in the Geant4 electron transport. Utilising the same setup as Ref.[2] we show the results of recent upgrades in the Geant4 electron transport algorithm.

The following section provides a description of the cavity setup and its simulation. Section 3 explains the key elements of electron transport in Geant4 and their parameters. Section 4 explains the revisions undertaken recently and studies the effect of varying the value of each parameter separately. In section 5 the different elements are combined, and the accuracy of the cavity response for transport is examined.

2. The Fano cavity setup

A new Geant4 application, the *FanoCavity* example[†], has been developed in order to test the different mechanisms involved in the electron transport: step limitation, energy loss fluctuation and multiple scattering.

The model of ionization chamber is the one described in [2] (Figure 1). The equilibrium condition for charged particles is realized using the beam regeneration technique. To force the equality of stopping power in wall and cavity, the density effect correction term is neglected and the bremsstrahlung process turned off. Some elements of biasing were introduced in the Compton process:

[†] This example is included in the Geant4 distribution.

the cross section is set to zero in the cavity to force conservation of the charged particle fluences, secondary particles which have no chance to reach the cavity are killed and statistics are further improved by increasing the cross section in the wall (by a factor of 1000 in the present work).

The electrons are tracked under the Continuous Slowing Down Approximation (CSDA). Thus there is no delta-electron production.

The error bars shown in the graphs in this paper represent the statistical errors based on the number of electrons entering the cavity (one-sigma uncertainty).

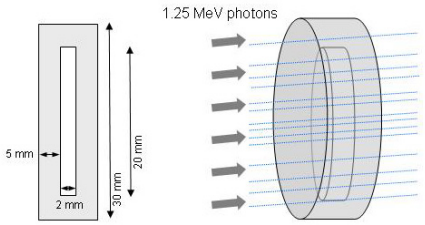

Figure 1 : the Fano cavity setup
A 1.25 MeV photon beam crossing an ionization chamber made of water (wall) and steam (cavity)

3. Description of the electron transport algorithms in Geant4

We give here a brief description of the parameters used for steering in the Geant4 electron transport algorithms [3-6], including parameters for step limitation, energy loss calculation and the multiple scattering process.

3.1. Basis of the step size limitation for an electron

Besides geometrical limits, the electron step size is limited by several competitive constraints.

The first limitation is due to the production threshold (*aka* cut) for ionization and bremsstrahlung. Under CSDA conditions this constraint does not apply.

The second limitation is related to the computation of the mean energy loss per step. A *Step function* is used which is controlled by two parameters: the maximum reduction of fraction of stopping range *dRoverRange* and the minimum range value *finalRange*. The step limitation is defined by:

$$\text{Step}/\text{Range} < dRoverRange \qquad \textbf{(1)}$$

The step size decreases gradually until the stopping range becomes lower than the *finalRange* value. In this case, the remaining range of an electron is done in one step. In this study the value of *finalRange* is set to 10 μm, which more or less corresponds to a tracking cut of 20 keV in water.

Multiple scattering [5] introduces an additional step limitation. This depends on the range and geometry and is controlled by three parameters: *RangeFactor*, *GeomFactor* and *skin*. The initial step limit is defined at the beginning of the track by:

$$\text{Step} = RangeFactor * \max(\text{Range}, \lambda) \qquad \textbf{(2)}$$

where λ is the transport mean free path derived from the multiple scattering model [5] and *Range* is an electron range. *RangeFactor* limits the maximum size of the step to a fraction of the particle mean free path or range. It is an internal parameter of the multiple scattering model which default value is 0.02. This step size limit is only recomputed after each boundary crossing.

The second parameter, *GeomFactor*, is applied to ensure that a minimum number of steps is done in any geometrical volume, independently of its thickness. This constraint is necessary to control the step size in a low density medium or for very thin layers. The step size is limited by *1/GeomFactor* of the linear distance to the next geometrical boundary. This limit is computed at a track's initial point

and recomputed only when entering a new volume. This limitation is usable only in the absence of a strong magnetic field. It is active only if the value of the parameter *skin* is above zero.

A single Coulomb scattering mode has been added in the scattering process in order to refine the calculation of the electron trajectory when crossing boundary. This was introduced in Geant4 release 8.2. The reason for this modification is to allow scattering to be sampled "in average", while near the boundary the condition for the applicability of multiple scattering is not satisfied. More details of this option and the related *skin* parameter are given in section 4.3 below.

3.2. Final state of an electron after one step

Once the step size for the electron has been determined, the multiple scattering process is invoked to compute the true path length *t*, which is larger than the distance between the initial and final points (Figure 2). The mean energy loss along this true path length is calculated, and then its fluctuation is sampled. Next the multiple scattering model is invoked again to compute the angular deflection and lateral displacement of the primary electron at the end point. If any interaction is happen at the end point, then a secondary particle is generated.

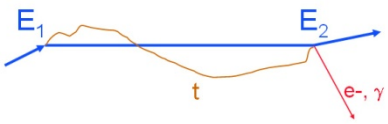

Figure 2 : description of a step

The final energy is calculated from the energy balance:

$$E_1 - E_2 = \langle \Delta E \rangle + dE + T_{kin} \qquad \textbf{(3)}$$

where : E_1, E_2 are the energies of the electron at the beginning and the end of the step

$<\Delta E>$ is the mean energy loss calculated for the path length *t*

dE is the energy loss fluctuation (this fluctuation can be positive or negative)

T_{kin} is the energy of the generated secondary (e- or γ), if any. Under the CSDA condition no secondaries are emitted, so $T_{kin} = 0$.

The relevant classes, helped by the modular Geant4 design, enable a user or a developer to isolate individual actions. For instance, we can enable or disable the multiple scattering process or the sampling of energy loss fluctuation.

4. Evolution of the electron transport algorithms in Geant4

Having defined the parameters and processes involved in electron transport, we now summarise the modifications provided in recent Geant4 releases and their effects.

4.1. Mean energy loss computation : <ΔE>

In Geant4 the mean energy loss is computed from range and inverse range tables in order to take into account the variation of stopping power along the step. In the case of small steps, this computation can become unstable and is replaced by a linear approximation (i.e. stopping power assumed constant). The limit of this approximation is controlled by the parameter *linLossLimit* :

$$\text{Step}/\text{Range} < linLossLimit \qquad \textbf{(4)}$$

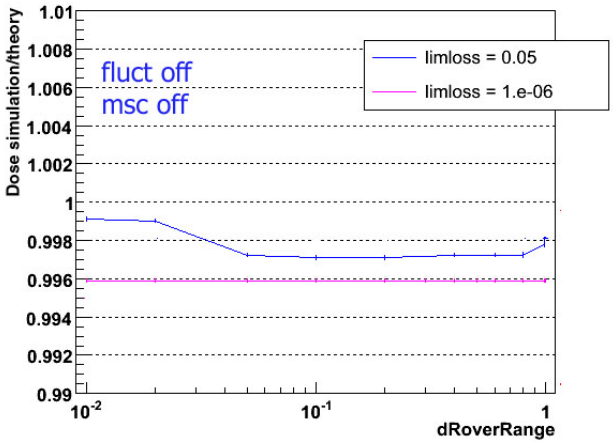

Figure 3 : response of the cavity (simulated dose deposition divided by the theoretical dose) versus the step limitation parameter *dRoverRange*

The existing default value of the parameter *linLossLimit* = 0.05 was chosen as a general transport parameters for any particle type. In this work a new value of 10^{-6} has been used which improves the numerical stability of results.

We made our preliminary study by switching off calculation of energy loss fluctuation and the multiple scattering process. Under these conditions the electron transport does not include any random mechanism, and is entirely governed by the parameter *dRoverRange* (for a given *finalRange* value). Figure 3 shows the stability of simulated and theoretical dose deposition in the cavity when varying *dRoverRange*. The cavity response in this and other plots is a ratio of simulated dose deposition inside the cavity to the theory based calculation of the dose using incoming gamma beam fluence. It is seen in Figure 3 that despite a systematic shift of ~0.004, which remains to be understood, the value of 10^{-6} for the *linLossLimit* parameter ensures numerical stability.

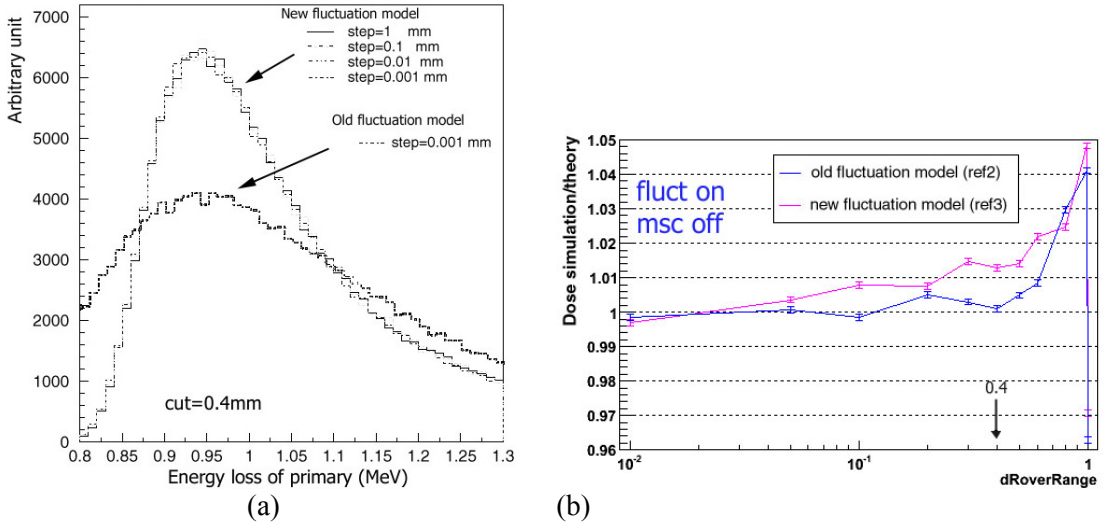

Figure 4 : (a) energy loss distribution of 15.7 MeV electrons in 4 mm of Be for various maximum step length
(b) Fano cavity test: comparison of Geant4 versions 8.2/8.3 (ref2/ref3) energy loss fluctuation models

4.2. Energy loss fluctuation computation: dE

The fluctuation model of Geant4 [6] depends on the material and the value of the production threshold (cut). Recent tests highlighted that this model was deficient for small amounts of matter, for example in the case of small steps or gas. An enhanced model is now implemented in Geant4 [4].

Figure 4a shows the energy loss distribution in 4 mm of Be for 15.7 MeV electrons for various step size limitations: from 1 mm to 1 μm. For step = 1 μm the energy distribution was significantly different with Geant4 version 8.2 (ref2). This disappears with the corrected model in Geant4 version 8.3 (ref3). Figure 4.b shows the Fano cavity response in the two cases. With the corrected model the stability is ~0.003 when the step size is constrained by dRoverRange < 0.4.

4.3. Improvements in the multiple scattering process

Starting with release 8.0, the multiple scattering has been revised in order to refine the step limitation methods, the description of boundary crossing and the angular distribution of scattered particles [4, 5].

Concerning the step limitation, new default values were defined for *RangeFactor* and *GeomFactor* (in the release 8.3 *RangeFactor* = 0.02, *GeomFactor* = 2.5).

Near boundaries (before and after), step size is small (~λ elastic) and approximate single Coulomb scattering is applied (Geant4 release 8.2). Based on the new *skin* parameter the thickness of the layer in which single Coulomb scattering is applied is defined by *λ*skin.*

Therefore *skin* is a number of elastic mean free path in which single scattering is applied (dimensionless floating number ≥ 1). The value *skin* = 0 disables the use of single scattering near boundaries. There is no upper limit for the parameter but, as will be shown below, a big *skin* value (~10) leads to single Coulomb scattering being applied at each step.

Work was also done to enhance the computation of lateral displacement by better evaluation of the safety radius. The isotropic safety is the distance from a given point to the nearest geometric boundary: it is estimated by the Geant4 geometry navigator. If the range of an electron is less than the safety, the current multiple scattering process does not impose a step limitation.

At the end of a step the scattering deflection angle and the radial displacement of the particle are sampled. The final direction is correlated with the lateral displacement according to Lewis's theory. Recently both the central parts and tails of the angular distribution have been fine-tuned [5]. All recent changes are documented in the Physics Reference Manual [4].

We have evaluated the influence of the *skin* parameter in the case of the Fano cavity application (Figure 5a). In this first calculation we turned off the energy loss fluctuations, in order to test the effect of the multiple scattering algorithm alone. The cavity response is stable already with *skin=1*.

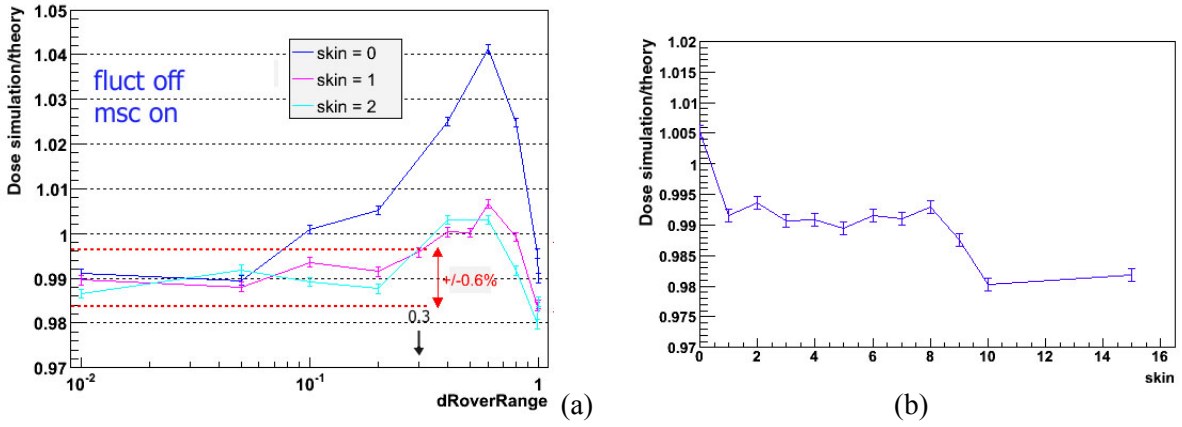

Figure 5 : study of the *skin* parameter (release 8.2-ref3)
(a) : cavity response versus *dRoverRange* for *skin* parameter values 0,1 and 2
(b) : cavity response versus *skin* parameter for *dRoverRange* = 0.2

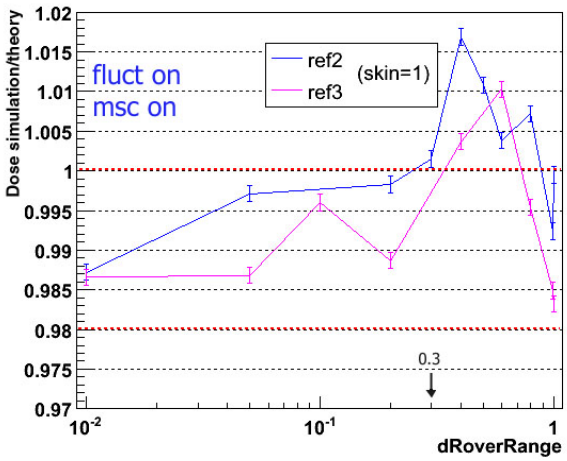

Figure 6 : responses of the cavity with upgraded fluctuation, multiple scattering algorithms and default parameters**.** The Geant4 version 8.2 referred to as ref2, the Geant4 version 8.3 as ref3.

Computations were undertaken for a set of *skin* values between 0 and 15 to evaluate an optimal default. Results are shown in Figure 5b for *dRoverRange* = 0.2. We note that the response stability decreases for a value of *skin* > 8. In this case the single Coulomb scattering is applied over a large thickness of medium. Since this model is approximate, it must not be applied to the whole trajectory. To get accurate results we must restrict this single Coulomb scattering model to regions closest to boundaries and keep multiple scattering elsewhere.

This study shows that the multiple scattering algorithm gives stable results with variation within 0.6%, if *skin* > 0 and *dRoverRange* < 0.3. The default value of *skin* is set to zero, however for precise simulation we would recommend the values 1 or 2.

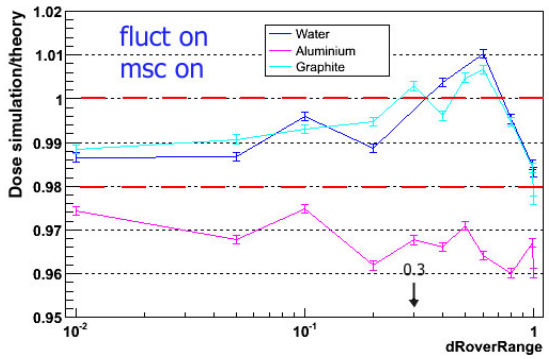

Figure 7 : response of the cavity with ionization chamber made of different materials

5. Geant4 release 8.3 and the Fano cavity application

In this section we present the results of the Fano cavity application when all the upgrades and modifications described above are applied.

Figure 6 shows the cavity response when both energy loss fluctuation and multiple scattering are active. The following simulation parameters were used: *RangeFactor* = 0.02, *GeomFactor* = 3 and *skin* = 1. On condition that *dRoverRange*<0.3, the results are stable within 1%. But a shift of ~1% is still observed.

To complete our study the computation has been done for other ionization chamber types characterized by a different material for both the wall and cavity. In the following examples, the material was replaced with aluminium in one case, and graphite in another (Figure 7).

Figure 8 shows that CPU time needed to execute the Fano cavity application depend on the *dRoverRange* parameter and practically not on the *skin.*

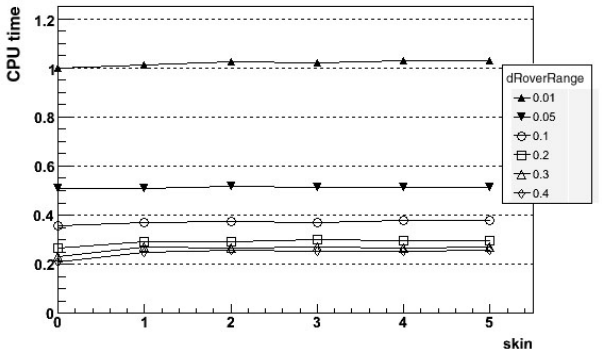

Figure 8 : Computation time (CPU time) Relative CPU time required for different values of the *skin* and *dRoverRange* parameters. Runs simulated 10^6 electrons crossing the cavity normalized to the time for the simulation with parameters (*skin*=0, *dRoverRange*= 0.01): about 350 s on Intel 2.66 GHz processor (Woodcrest 5150)

6. Conclusion and perspectives

Several improvements have been made in the Geant4 code concerning electron transport algorithms which have been analyzed in the context of the Fano cavity setup.

The stability of the mean energy loss computation has been improved to a level ~0.2% for this setup. The energy loss fluctuation algorithm has been tuned for very small amount of matter: its stability is now ~0.3% for a large range of step size limitation.

The revised multiple scattering algorithm significantly constrains the step size. The single Coulomb scattering model is applied near geometric boundaries. Hence the stability is ~ 1.5% for values of *dRoverRange* < 0.3. To achieve higher stability and precision below the 1% level, additional work is underway to understand the systematic shifts and to study the effects of other parameters.

The development and upgrades of the Geant4 toolkit described in this paper are available to Geant4 users with Geant4 8.3 release. The code of the Fano cavity example used in this work is publicly available as a Geant4 extended example, in the *fanoCavity* directory of medical examples.

7. Acknowledgments

We wish to thank Emily Poon and Frank Verhaegen for helpful discussions and our Geant4 colleagues for their encouragement. A special thanks to John Apostolakis and Ian McLaren for help with this note.

8. References

[1] Kawrakow I 2000 Accurate condensed history Monte Carlo simulation of electron transport. II. Application to ion chamber response *Med. Phys.* **27-3** 499

[2] Poon E, Seuntjens J and Verhaegen F 2005 Consistency test of electron transport algorithm in the Geant4 Monte Carlo code *Phys. Med. Biol.* **50** 681

[3] Agostinelli S *et al.* 2003 *NIM-A* **506** 250

[4] Geant4 Physics Reference Manual, Release 9.0, 30th June 2007, available at URL http://cern.ch/geant4/support/userdocuments.shtml

[5] Urban L 2006 A multiple scattering model in Geant4 *Preprint* CERN-OPEN-2006-077

[6] Lassila-Perini K and Urban L 1995 *NIM-A* **362** 416.